Neurobiology of Disease 130 (2019) 104494

Contents lists available at ScienceDirect

Neurobiology of Disease

journal homepage: www.elsevier.com/locate/ynbdi

Knockout of *latrophilin-3* in Sprague-Dawley rats causes hyperactivity, hyper-reactivity, under-response to amphetamine, and disrupted dopamine markers

Samantha L. Regan[a], Jillian R. Hufgard[b], Emily M. Pitzer[a], Chiho Sugimoto[c], Yueh-Chiang Hu[d], Michael T. Williams[c], Charles V. Vorhees[c,*]

[a] Neuroscience Graduate Program, University of Cincinnati, United States of America
[b] Department of Obstetrics and Gynecology, Indiana University School of Medicine, United States of America
[c] Department of Pediatrics, University of Cincinnati College of Medicine, Division of Neurology, Cincinnati Children's Hospital Medical Center, United States of America
[d] Department of Pediatrics, University of Cincinnati College of Medicine, Division of Developmental Biology, Cincinnati Children's Hospital Medical Center, Cincinnati, OH 45229, United States of America

ARTICLE INFO

Keywords:
Latrophilin-3 (LPHN3 or ADGRL(3))
ADHD
Dopamine D1 receptor (DRD1)
Tyrosine hydroxylase
Aromatic amino acid decarboxylase (AADC)
DARPP-32
Dopamine transporter (DAT)

ABSTRACT

Attention deficit hyperactivity disorder is a pervasive developmental disorder characterized by inattention, impulsivity, and hyperactivity and is 75–90% heritable. *Latrophilin-3* (*LPHN3;* or *ADGRL(3)*) is associated with a subtype of ADHD, but how it translates to symptoms is unknown. LPHN3 is a synaptic adhesion G protein coupled receptor that binds to fibronectin leucine rich transmembrane protein 3 and teneurin-3 (FLRT3 and TEN-3). We created a null mutation of *Lphn3* (KO) in Sprague-Dawley rats using CRISPR/Cas9 to delete exon-3. The KO rats had no effects on reproduction or survival but reduced growth. KO females showed catch-up weight gain whereas KO males did not. We tested WT and KO littermates for home-cage activity, anxiety-like behavior, acoustic startle response, and activity after amphetamine challenge. Expression of *Lphn3*-related genes, monoamines, and receptors were determined. *Lphn3* KO rats showed persistent hyperactivity, increased acoustic startle, reduced activity in response to amphetamine relative to baseline, and female-specific reduced anxiety-like behavior. Expression of *Lphn1*, *Lphn2*, and *Flrt3* by qPCR and their protein products by western-blot analysis showed no compensatory upregulation. Striatal tyrosine hydroxylase, aromatic L-amino acid decarboxylase (AADC), and the dopamine transporter were increased and dopamine D1 receptor (DRD1) and dopamine- and cAMP-regulated neuronal phosphoprotein (DARPP-32) decreased with no changes in DRD2, DRD4, vesicular monoamine transporter-2, *N*-methyl-D-aspartate (NMDA)-NR1, -NR2A, or -NR2B. LPHN3 is expressed in many brain regions but its function is largely unknown. Data from human, mouse, zebrafish, Drosophila and our new *Lphn3* KO rat data collectively show that its disruption is significantly correlated with hyperactivity and associated striatal changes in dopamine markers.

1. Introduction

Attention deficit hyperactivity disorder (Demontis et al., 2019) is a neurodevelopmental disorder characterized by hyperactivity, inattention, and impulsivity (Acosta et al., 2011), often with comorbid conditions, such as anxiety (Steinberg and Drabick, 2015; Tung et al., 2016). ADHD affects 5% of children and adolescents world-wide (Martinez et al., 2011) and 2.5% of adults (Franke et al., 2012; Demontis et al., 2019). Research has implicated dysregulation of monoamines, especially dopamine (DA) as important factors in ADHD (Sagvolden et al., 1998; Russell et al., 2005). Family, twin, and adoption studies indicate that ADHD is heritable, but it is not associated with large-effect gene variants, but rather with multiple small-effect variants (Hwang et al., 2015; van der Voet et al., 2016). ADHDGene lists 398 copy number variants, 1391 SNPs, and 173 gene associations from a genome-wide association study (GWAS), and linkage disequilibrium, pathway analyses, and gene mapping studies (Zhang et al., 2012). A new GWAS further reports a number of novel genetic associations with ADHD symptoms (Demontis et al., 2019).

GWAS and fine mapping studies from a genetic isolate in Colombia (Paisa) identified a heretofore unrecognized haplotype associated with ADHD: *latrophilin-3* (Arcos-Burgos and Muenke, 2010; Acosta et al.,

* Corresponding author at: Div. of Neurology, Cincinnati Children's Research Foundation, 3333 Burnet Ave., Cincinnati, OH 45229, United States of America.
E-mail address: charles.vorhees@cchmc.org (C.V. Vorhees).

https://doi.org/10.1016/j.nbd.2019.104494
Received 5 February 2019; Received in revised form 3 May 2019; Accepted 5 June 2019
Available online 06 June 2019

2011), also known as adhesion G protein-coupled receptor L(3) or *ADGRL(3)* [OMIM 616417]. Variants of *LPHN3* increase the risk of ADHD by 1.2 fold and are associated with symptom severity and medication response. The association was also found in North American, European, Spanish, Korean, and Chinese patients (Domene et al., 2011; Franke et al., 2012; Hwang et al., 2015; Huang et al., 2018). Twenty-one *LPHN3* SNP variants are associated with ADHD (Domene et al., 2011) and with response to methylphenidate, a common ADHD medication (Arcos et al., 2010; Ribases et al., 2011; O'Sullivan et al., 2014; Hwang et al., 2015; Ranaivoson et al., 2015). *LPHN3* is also associated with substance abuse disorders, another comorbidity with ADHD (Arcos-Burgos et al., 2019).

Latrophilins are adhesion G protein coupled receptors (aGPCRs). There are three isoforms: LPHN1 is expressed in brain and periphery; LPHN2 is primarily peripheral, and LPHN3 is in brain and adrenal (Sugita et al., 1998). LPHN3 is most abundant in caudate-putamen, but is also expressed in prefrontal cortex (PFC), amygdala, hippocampus (HIP), and cerebellum (Cb) (Arcos et al., 2010). LPHN3 is localized synaptically with an extracellular domain that binds to fibronectin leucine rich transmembrane protein (FLRT3) and teneurin-3 (Sando et al., 2019) thereby spanning the synaptic cleft. The LPHN3-FLRT3-teneurin-3 linkage is also associated with adjacent residues forming a synapse spanning linkage composed of a dystroglycan-teneurin complex cross-linked at a TCAP site. This complex is thought to stabilize the synapse (Silva and Ushkaryov, 2010; Ranaivoson et al., 2015) and determine synaptic specificity (Sando et al., 2019).

Knock-down of the *lphn3.1* orthologue in zebrafish leads to increased swim distance and speed, and the effects are reversed by methylphenidate (MPH), atomoxetine (ATO), and selective dopaminergic agonists; also the number of DA cells were reduced in the posterior tuberculum (Lange et al., 2012; Lange et al., 2018). *Lphn3* knockout (KO) mice are hyperactive in a novel environment and show exaggerated hyperactivity when given cocaine. These mice also have increased brain DA and serotonin (5-HT) (Wallis et al., 2012) and a complex pattern of protein expression changes (Orsini et al., 2016). Knockout of *lphn3* in *Drosophila* similarly causes hyperactivity that is reduced by methylphenidate (van der Voet et al., 2016). However, little is known about LPHN3 beyond the hyperactivity induced by its deletion. To address this, we used CRISPR/Cas9 to delete exon 3 of *Lphn3* in Sprague-Dawley rats. We hypothesized that these rats would not only show acute hyperactivity, but persistent hyperactivity in a familiar environment, a key feature of ADHD (Russell et al., 2005). We further hypothesized that LPHN3 deletion would increase startle reactivity and reduce motor activation in response to amphetamine, and these changes would be accompanied by changes in DA markers.

2. Methods

2.1. Animals and husbandry

2.1.1. Generation of Lphn3 KO rats

Lphn3$^{-/-}$ (knockout) rats on a Sprague-Dawley (CD-IGS, strain 001, Charles River, Charleston, NC) background were generated in the Cincinnati Children's Transgenic Animal and Genome Editing Core using CRISPR/Cas9 to delete exon 3 (Fig. 1A). Briefly, two sgRNAs targeting the sequences flanking exon 3 (GTCCCTTGCCAGTACATCTC and CCTAGTGTTGTGTTCTGCTA) were selected according to the off-target scores from the CRISPR design web tool (http://genome-engineering.org). The sgRNA and Cas9 mRNA were in vitro transcribed using MEGAshorscript T7 kit (ThermoFisher) and mMESSAGE mMACHINE T7 ULTRA kit (ThermoFisher), respectively, according to the manufacturer's instructions. The mutant rats were generated by injection of two sgRNAs (50 ng/μL each) and Cas9 mRNA (100 ng/μL), along with two ssDNA donor oligos that contained loxP (50 ng/μL each), into the cytoplasm of fertilized eggs, using a piezo-driven microinjection technique (Yang et al., 2014; Scott and Hu, 2019). Injected embryos were transferred immediately into the oviductal ampulla of pseudopregnant females. Live born pups were genotyped by PCR and further confirmed by Sanger sequencing. We obtained several KO alleles though the loxP-containing alleles were not obtained from this round of microinjection. We bred the founders with wildtype (WT) rats to establish the lines and used *Lphn3*$^{+/-}$ × *Lphn3*$^{+/-}$ crossings for generating KO and WT littermates for the experiments (Olincy et al., 2000). Rats were housed in polysulfone cages in a pathogen free vivarium using a Modular Animal Caging System (Alternative Design, Siloam Spring, AR) with HEPA filtered air at 30 air changes/h (Alternative Design, Siloam Spring, AR). Rats were provided ad libitum reverse-osmosis filtered/UV sterilized water (SE Lab Group, Napa, CA) and fed NIH-07 rat chow (LabDiet, Richmond, IN). Cages had woodchip bedding and stainless steel huts as enrichment (Vorhees et al., 2011). Rats were maintained on a 14 h light-10 h dark cycle (lights on at 600 h) at 20 ± 1 °C and 50 ± 10% relative humidity. Multiparous *Lphn3*$^{+/-}$ × *Lphn3*$^{+/-}$ pairs were bred, and pregnant dams were moved to individual cages. Birth was designated postnatal day 0 (P0). Ear punches were collected from offspring at P7 for genotyping using three primers: 1. AAAGGGTCATAGCATCCGGC, 2. CTAACGTGGCTTTTTGTCTTCT, and 3. GCTCGACAGACAGTGTGGAT. HotStarTaq Master Mix kit (Qiagen, Hilden, Germany) was used per manufacturer recommendations. Thermocycler parameters were: 1) 95 °C 5 min, 2) 94 °C 1 min, 3) 61.5 °C 1 min, 4) 72 °C 2 min, 5), steps 2–4 were repeated 34 more times followed by 6) 72 °C 10 min, and 7) held at 4 °C until the product was run on a 2% agarose gel with ethidium bromide staining. The WT band occurs at ~320 bp and KO band at ~452 bp. (Fig. 1B).

Dams were removed from litters on P28, and offspring were housed 2/cage/sex. Offspring were tested for 48 h of home-cage activity on P35 and again at P50 followed by tests for anxiety, acoustic startle response, and activity with amphetamine challenge. To control for litter effects, only one rat per genotype per sex was tested per litter and selected using a random number table. Testing was by personnel blinded to the genotype. The vivarium is accredited by AAALAC International. All research followed the NIH Guide for the Care and Use of Animals in Research. Protocols were approved by the Cincinnati Children's Research Foundation Institutional Animal Care and Use Committee.

2.2. Behavioral tests

20 WT male, 20 WT female, 20 KO male, and 20 KO female rats from 20 litters were used. Home-cage activity was assessed on P35–36 and P50–51. On P52 rats were tested in an elevated zero maze (EZM) for 5 min. On P53 rats were tested for acoustic and tactile startle (ASR/TSR). On P60 rats were tested acutely for open-field activity before and after a challenge dose of amphetamine. Rats were later euthanized and brains dissected into hippocampus (HIP), neostriatum (STR), nucleus accumbens (NAcc), prefrontal cortex (PFC), and cerebellum (Cb) over ice and stored at −80 °C. Behavioral equipment was cleaned between subjects with Process NPD cleaner (STERIS Life Sciences, Mentor, OH) an EPA approved, non-toxic denaturing, antibacterial, antiviral solution.

2.2.1. Home-cage activity

Rats were singly housed for 48 h during home-cage activity testing (Tang et al., 2002). Each cage rested within a frame consisting of a 4 × 8 array of photocells spaced 5 cm apart located along the X and Y axes 2 cm above the bottom of the cage (PAS System, San Diego Instruments, San Diego, CA).

2.2.2. Elevated zero maze

Anxiety-related behavior was measured using an EZM. The maze was a circular track 10 cm wide, 100 cm in diameter, and elevated 50 cm from the floor (Stoelting Co., Wood Dale, IL). The floor is made of gray texturized aluminum. The maze was divided in four quadrants of

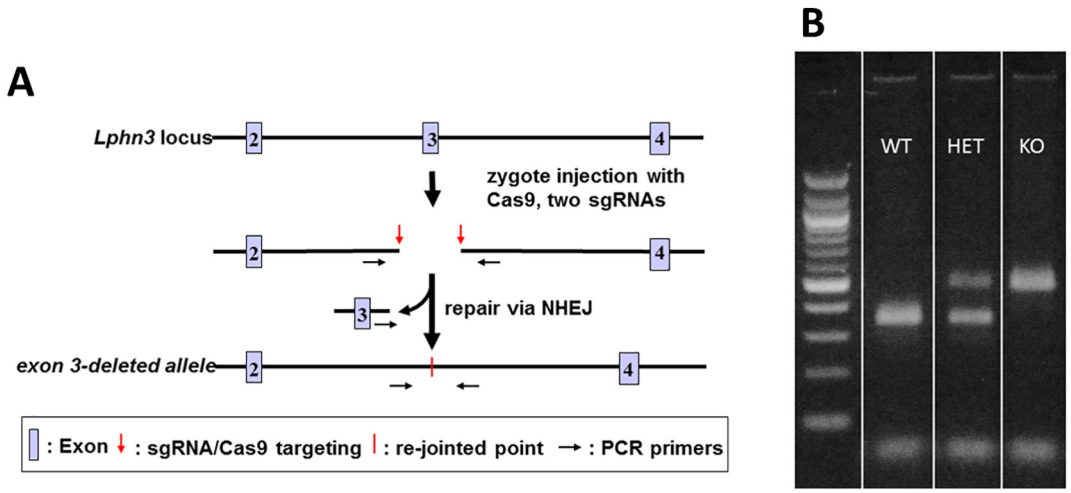

Fig. 1. CRISPR/Cas9 targeting strategy and PCR genotypes. A. Illustration of region targeted by sgRNA excising exon 3. B. PCR genotyping bands indicating WT in lane 2, HET in lane 3, and the KO band in lane 4.

equal size with two open and two closed quadrants. Open quadrants had 1.3 cm high clear acrylic curbs to prevent falls, and the two opposing closed quadrants had 30 cm high acrylic walls with inner walls of IR transparent acrylic. Testing was performed under 8.2 lx. Rats were placed in the middle of a closed quadrant and allowed to explore for 5 min. A camera mounted above the maze was synchronized to a computer in an adjacent room with Any-maze tracking software (Stoelting Co., Wood Dale, IL).

2.2.3. Startle response

Acoustic (ASR) and tactile startle responses (TSR) were measured in SR-LAB apparatus (San Diego Instruments, San Diego, CA). Each rat was placed in an acrylic cylindrical holder mounted on a platform with a piezoelectric accelerometer mounted underneath. The holder was placed inside a sound-attenuated chamber with fan and house light. Each session consisted of a 5 min acclimation period followed by 50 trials of each type. The acoustic pulse was a 20 ms 120 dB sound pressure level mixed frequency white noise burst (rise time 1.5 ms), and the tactile burst was a 20 ms, 50 psi air puff directed at mid-dorsum. The recording window was 100 ms. Maximum and average startle amplitude (V_{max} and V_{avg} (both in mV)) were analyzed in blocks of 10 trials.

2.2.4. Open-field with amphetamine challenge

Rats were placed in 41 × 41 cm activity monitors (PAS System, San Diego Instruments, San Diego, CA) with 16 photocells spaced along the X and Y planes positioned 2 cm above the floor. Rats were first habituated for 30 min to the test chamber. They were then removed and injected s.c. with saline (1 mL/kg) and further tested for 30 min such that they were at basal levels of activity. Following this, they were removed, administered s.c. (+)-amphetamine sulfate (1 mg/kg in 1 mL/kg saline, expressed as the freebase and > 99% purity, Sigma-Aldrich), and tested for an additional 180 min. Activity was captured in 5-min intervals and analyzed in 10-min intervals.

2.3. Monoamines

After a one week washout period, rats were euthanized, brains dissected over ice, frozen on dry ice, and stored at −80 °C. For assay, tissue was weighed and sonicated in 0.1 N perchloric acid and centrifuged at 2100 RCF for 13 min at 4 °C. The supernatant (20 µL) was collected and loaded on a Dionex UltiMate® 3000 analytical autosampler (Thermo Scientific) for injection into a high performance liquid chromatograph (HPLC) with an electrochemical detector (ECD). The HPLC-ECD system consisted of an ESA 5840 pump, an ESA 5020 Guard Cell, a Supelco Supelcosil™ LC-18 column (15 cm × 4.6 mm, 3 µm, Sigma-Aldrich Co.) and a Coulochem III ECD (Thermo Fisher Scientific). The pump flow rate was 0.5 mL/min at 28 °C. Potential for the guard cell was +350 mV and the Coulochem III potential settings were − 150 mV for E1 and + 250 mV for E2. Commercially available MD-TM mobile phase (Thermo Fisher Scientific) consisting of 89% water, 10% acetonitrile, and 1% sodium phosphate monobasic (monohydrate) with pH = 3 was used. Standards for norepinephrine (NE), DA, 5-HT, 3,4-dihydroxyphenylacetic acid (DOPAC), 5-hydroxyindoleacetic acid (5-HIAA), and homovanillic acid (HVA) were prepared in 0.1 N perchloric acid. All neurotransmitter standards were run on a single chromatogram as well as individually for peak verification. Neurotransmitter standards were run with serial dilutions in order to produce a standard curve.

2.4. Quantitative PCR

RNA was isolated from STR and PFC from 8 KO and 8 WT male rats using RNAqueous-Micro (ThermoFisher Scientific) following the manufacturer's instructions. RNA was isolated using 1 mL of TRIzol for every 50–100 mg of tissue. RNA was quantified by Nanodrop (Thermo Scientific). Reverse transcription (RT) reactions were performed using 4 µL of iScript at room temperature with 1 µg-1 pg of RNA template (Bio-Rad) in a final volume of 20 µL. PCR reactions were carried out as follows: 5 min at 25 °C, 20 min at 46 °C, and 1 min at 95 °C. Quantitative PCR (qPCR) samples contained 160 ng of cDNA, 300 nM of each primer (forward and reverse), and 1× SYBR Green Master Mix (BioRad) in a 20 µL volume. Two 20 µL aliquots of the mix were placed in a 96-well plate and the qPCR was performed on an 7500 Real Time PCR System (Applied Biosystems) using the following conditions: 50 °C for 2 min, 95 °C for 10 min, 50 cycles at 95 °C for 15 s, and 60 °C for 1 min. Primers were synthesized by Integrated DNA Technologies (Coralville, IA) and selected based on primer efficiency at 95–100%. Rat primer sequences are shown in Table 1. Ct values were determined using Applied Biosystems 7500 System Sequence detection software (v2.4) with a threshold set at 0.5. The average Ct values from duplicates assayed were calculated. Changes in mRNA were measured with the ΔΔCt method (Livak and Schmittgen, 2001) using actin as the reference and the *Lphn3* WT rat samples as calibrator.

2.5. Western Blots

Western blots were used to confirm LPHN3 deletion and analyze DA

Table 1
qPCR primers.

Gene	Primer Sequence (5′- > 3′)
Lphn1	CTCTGCTACCCAAGGCCTGA
	CCACACACTGGGTTCGGTTA
Lphn2	TCTGGTACACAGAGCCGTA
	GGGGTCGAAGAAGAGGGTTT
Lphn3	ACCCCATTGAGCTACGCTGT
	ATCTTGTCATCTGTCCTCCCG
Flrt3	TCTTCCTGGAGGTGCTCAGTC
	TCATGGTCAGCAGTGTTGAGG

markers in STR from 8 WT and 8 KO female rats; actin was used as a reference (Fig. 3D–G). Frozen tissue was homogenized in radioimmunoprecipitation assay buffer (25 mM Tris, 150 mM NaCl, 0.5% sodium deoxychlorate, and 1% Triton X-100 adjusted to 7.2 pH with protease inhibitor (Pierce Biotechnology, Rockford, IL). Protein was quantified using the BCA™ Protein Assay Kit (Pierce Biotechnology, Rockford, IL) and diluted to 3 µg/µL. Western blots were performed using LI-COR Odyssey® (LI-COR Biosciences, Lincoln, NE) procedures. Briefly, 25 µL of sample was mixed with Laemmli buffer (Sigma, USA) and loaded on a 12% gel (Bio-Rad Laboratories, Hercules, CA) and run at 200 V for 35 min in running buffer (25 mM Tris, 192 mM glycine, 0.1% sodium dodecyl sulfate (SDS)). The gel was transferred to Immobilon-FL transfer membrane (Millipore, USA) in 1× rapid transfer buffer (AMRESCO, Solon, OH) at 40 V for 1.5 h. Membranes were soaked in Odyssey phosphate buffered saline blocking buffer for 1 h and incubated overnight at 4 °C with primary antibody in blocking buffer with 0.2% Tween 20. Membranes were incubated with secondary antibody in blocking buffer (0.2% Tween 20 and 0.01% SDS) for 1 h at room temperature. Antibodies were mouse anti-LPHN3 (SC-393576, Santa Cruz Biotechnology, Dallas, TX) at 1:500, and 1:15,000 rabbit anti-actin (926-42210, LI-COR Biosciences, Lincoln, NE). Odyssey IRDye 680 secondary antibody was used at a 1:15,000 dilution (LI-COR Biosciences, Lincoln, NE). Rabbit anti-tyrosine hydroxylase (TH) (Ab112, AbCam, Cambridge, MA) at 1:1000 with Odyssey IRDye 800 secondary body used at a 1:2000 dilution. Rabbit anti-dopamine transporter (DAT) (Ab184451, AbCam, Cambridge, MA) at 1:2000 with Odyssey IRDye 800 secondary antibody at 1:20,000 dilution. Rabbit anti-dopamine receptor D1 (DRD1) (Ab40653, AbCam, Cambridge, MA) at 1:1000 with Odyssey IRDye 800 secondary antibody at 1:3000 dilution. Rabbit anti-dopamine receptor D2 (DRD2) (Ab85367, AbCam, Cambridge, MA) at 1:500 with Odyssey IRDye 800 secondary antibody at 1:3000 dilution. Rabbit anti-dopamine receptor D4 (DRD4) (SC-33661, Santa Cruz Biotechnology, Dallas, TX) at 1:500, and 1:15,000 rabbit anti-actin (926–42,210, LI-COR Biosciences, Lincoln, NE) with Odyssey IRDye 680 secondary antibody at 1:5000 dilution. Rabbit anti-DOPA decarboxylase (aromatic amino acid decarboxylase) antibody (Ab3905, AbCam, Cambridge, MA) at 1:1000 with Odyssey IRDye 800 secondary antibody at 1:2000 dilution. Rabbit anti-DARPP32 (Ab40801, AbCam, Cambridge, MA) at 1:2000 with Odyssey IRDye 800 secondary antibody at 1:4000 dilution. Mouse anti-actin (Ab3280, AbCam, Cambridge, MA) at 1:2000 with Odyssey IRDye 680 at a 1:15,000 secondary antibody as a loading control. Because of the known interactions between DA and NMDA neurons, western blot analyses were performed for subunits of the NMDA receptors (de Bartolomeis et al., 2014). Rabbit anti-NMDA receptor 1 (NR1) (Ab109182, AbCam, Cambridge, MA) at 1:4000 with Odyssey IRDye 800 secondary antibody at 1:3000 dilution. Rabbit anti-NMDA receptor 2A (NR2A) (Ab124913, AbCam, Cambridge, MA) at 1:9000 with Odyssey IRDye 800 secondary antibody at 1:20,000 dilution. Rabbit anti-NMDA receptor 2B (NR2B) (Ab81271, AbCam, Cambridge, MA) at 1:5000 with Odyssey IRDye 800 secondary antibody at 1:20,000 dilution. Rabbit anti-vesicular monoamine transporter 2 (AB1598P, Millipore, Temecula, CA) at 1:1000 with Odyssey IRDye 800 secondary antibody at 1:2000 dilution. Relative protein levels were quantified using the LI-COR Odyssey® scanner and Image Studio software for fluorescent intensity of each sample normalized to actin.

2.6. Experimental design and statistical analysis

Data were analyzed using general linear model ANOVAs (SAS, v9.3, SAS Institute, Cary, NC) with $p \leq .05$ as the threshold for significance. To control for litter effects, only one rat per genotype per sex per litter was used, and litter was used as a random factor in ANOVAs. Two-factor mixed model ANOVAs were used when between-subject factors were genotype and sex with Kenward-Rogers degrees of freedom. Repeated measure (RM)-ANOVAs for activity with time or weight with day as repeated measure factors used autoregressive moving average RM-ANOVA (ARMA(1,1) mixed models with first order Kenward-Roger degrees of freedom. *t*-tests for independent samples were used for qPCR and western data. Open-field activity was log transformed to normalize the data.

3. Results

3.1. Lphn3 KO characteristics

Lphn3 KO rats showed no apparent differences in gross appearance, survival, grooming, and had no outward signs of differences compared with WT rats. *Lphn3* KO male rats had reduced weight gain that was significant by P28 and remained lower through the end of the experiment at P91 (Fig. 2A). KO females had less weight gain than WT females from P21-P84, but showed no differences at P91 [Genotype: ($F(1,72) = 57.24$, $p < .0001$); Day: ($F(13,832) = 658.54$, $p < .0001$); Genotype × Day: ($F(13,832) = 5.19$, $p < .0001$); Sex: ($F(1,84.3) = 196.21$, $p < .0001$); Sex × Genotype: ($F(1,69.1) = 6.53$,

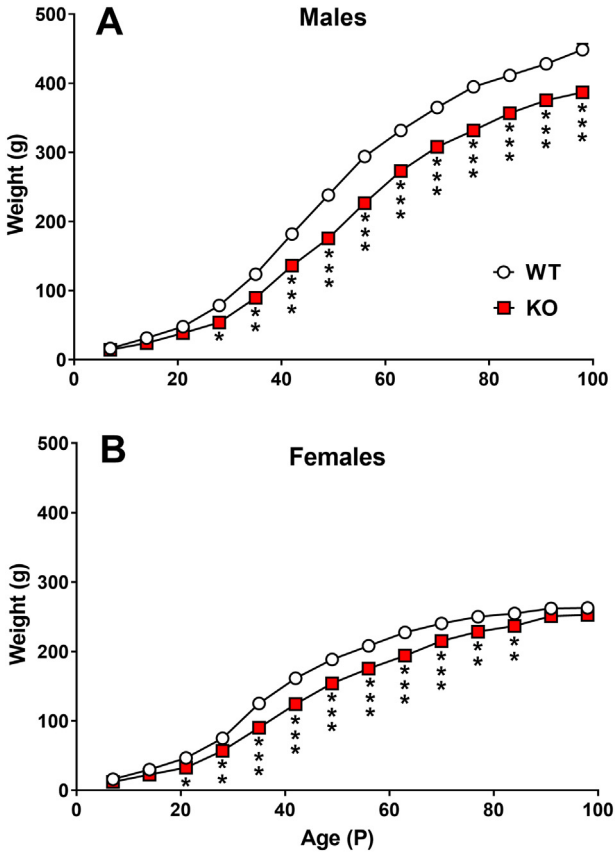

Fig. 2. Growth of Lphn3 KO and WT rats. A. Growth of males. B. Growth of females. Group sizes: Male: WT $n = 19$, KO $n = 20$; female: WT n = 20, KO $n = 20$. $^{*}P < .05$; $^{***}P < .001$ vs. WT.

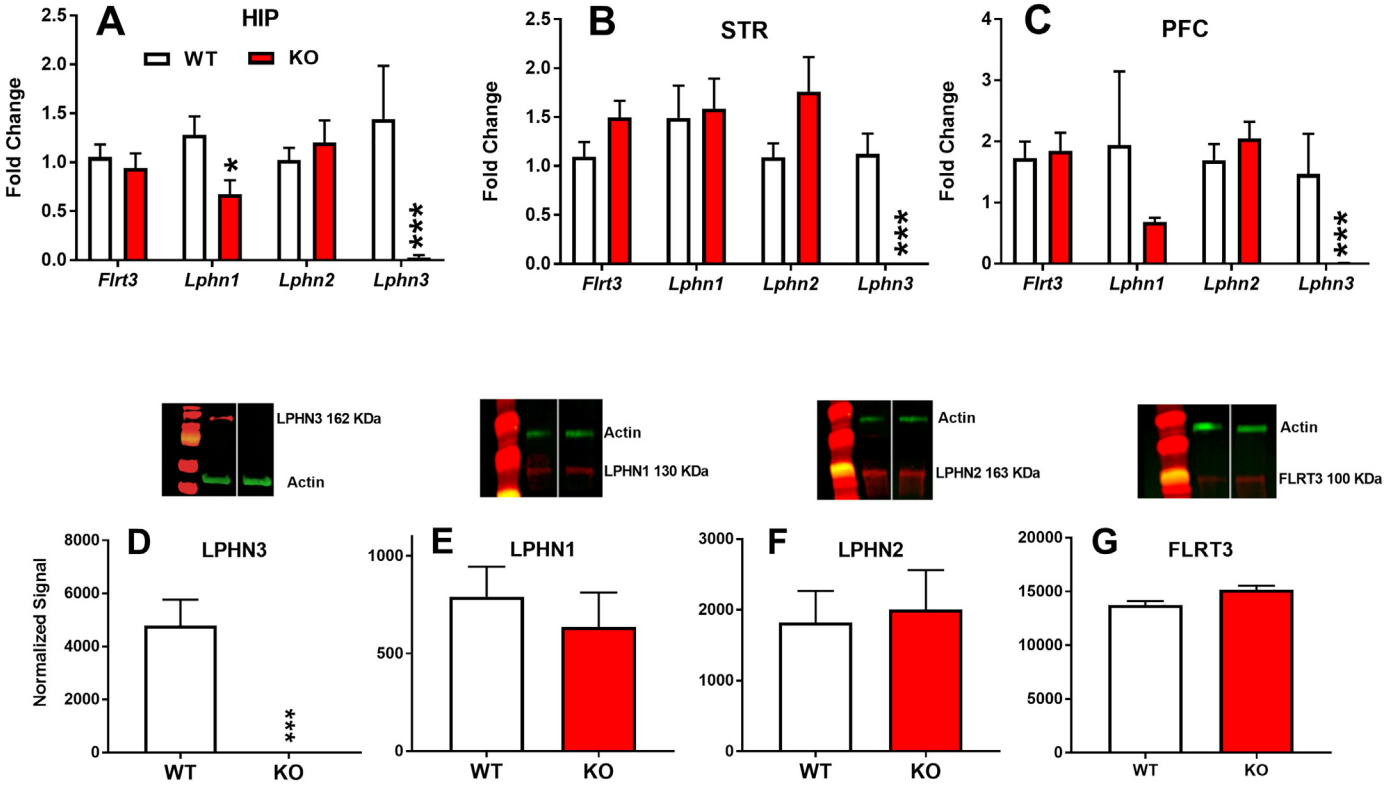

Fig. 3. Gene and protein expression in Lphn3 KO and WT littermates. *Lphn3* mRNA was undetectable in HIP, STR, and PFC (A–C). In HIP there was a reduction in *Lphn1* mRNA (A). There were no changes in *Lphn1*, *Lphn2*, or *Flrt3* in STR (B) or PFC (C). Protein expression by western blot in STR showed no detectable levels of LPHN3 (D) and no differences for LPHN1, LPHN2, or FLRT3 (E, F, G, respectively). Group sizes (males): STR: WT n = 7–8, KO n = 7–8). HIP: WT n = 8, KO n = 8). PFC: WT n = 8, KO n = 7–8. $^{*}p \leq .05$; $^{***}p \leq .001$ vs. WT.

$p < .0128$); Sex × Day: (F(13,832) = 46.20, $p < .0001$); Genotype × Sex × Day: (13,832) = 2.36, $p < .0042$)] (Fig. 2B).

3.2. mRNA and protein analysis

Deletion of exon 3 resulted in absence of *Lphn3* mRNA expression in HIP [t(7.1) = −2.6, $p = .01$], STR [t(7.0) = −5.41, $p = .0001$], and PFC [t(7.0) = −2.21, $p = .04$] (Fig. 3A–C) of KO rats compared with WT littermates. Within the HIP, *Lphn1* mRNA was reduced [t(12.5) = −2.56, $p = .02$] (Fig. 3A). No changes were found for *Lphn2* or *Flrt3* in HIP] or for *Lphn1*, *Lphn2*, or *Flrt3* in STR (Fig. 3B) or PFC (Fig. 3C).

LPHN3 protein was absent in STR of KO rats [t(10) = 5.0, p = .0001] (Fig. 3D), whereas there were no changes in LPNH1 (Fig. 3E), LPHN2 (Fig. 3F) or FLRT3 (Fig. 3G) compared with WT rats.

DA- and NMDA-related proteins were examined in the STR. TH [t(17) = 2.3, $p = .034$) (Fig. 4A)], AADC [t(10) = 2.39, $p = .0383$ (Fig. 4B)], and DAT [t(9.63) = 3.14, $p < .01$ (Fig. 4C)] were significantly increased, whereas DRD1 was reduced (Fig. 4D) [t(22) = −2.41, $p < .025$] in KO rats compared with WT rats. DARPP-32 also showed a significant reduction [t(13.23) = −3.89, $p < .002$] (Fig. G) in *Lphn3* KO rats compared with WT rats. No differences were seen in DRD2, DRD4, VMAT-2, NMDA-NR1, NMDA-NR2A, or NMDA-NR2B between KO and WT rats (Fig. 4E, F, H–K).

3.2.1. Home-cage activity

At P35, KO male and female rats exhibited hyperactivity compared with WT rats (Fig. 5A, B) [P35: Genotype: (F(1,340) = 57.42, $P = .0001$)]. Other significant outcomes were Sex: ($p < .0091$) females were more active than males; Interval: ($p < .0001$); and Genotype × Interval: ($p < .0001$). At P50 a similar pattern was seen: Genotype was significant (F(1,264) = 16.63, $p = .0001$). Other significant outcomes were Sex: ($p < .0001$) females were more active than males, Interval ($p < .0001$); Genotype × Interval ($p < .0001$), and Sex × Interval: ($p < .0001$). Hyperactivity appeared during the first diurnal period in KO rats, then declined to WT levels before reemerging during the dark cycle. During the second light cycle hyperactivity in KO rats continued but gradually declined to WT levels before the start of the second dark cycle when the hyperactivity emerged again, and this continued throughout the dark period and gradually declined again during the third light period.

3.3. Elevated zero maze

There was no main effect of genotype, but there was a main effect of Sex: (F(1,69.5) = 8.73, $p = .0043$), females spent more time in the open than males. There was an interaction of Genotype × Sex: (F(1,50.9) = 8.21, $p = .006$), and the genotype effect was only in females with the KO females in the open more than the WT females: ($p = .0021$); no differences were seen in males (Fig. 6A).

3.3.1. ASR/TSR

The KO rats had an increased ASR compared with the WT rats [Genotype: (F(1,62.1) = 30.46, p = .0001)] (Fig. 6B); Block was also significant ($p < .0001$).

There was no genotype main effect for TSR but there was a significant Genotype × Block: (F(4,295) = 2.74, $p = .0291$). KO rats were more reactive on all blocks compared with WT rats, but only block-5 was significant (Fig. 6C).

3.4. Locomotor with amphetamine challenge

During habituation, KO rats showed increased central and peripheral open-field activity compared with WT littermates, i.e., for central

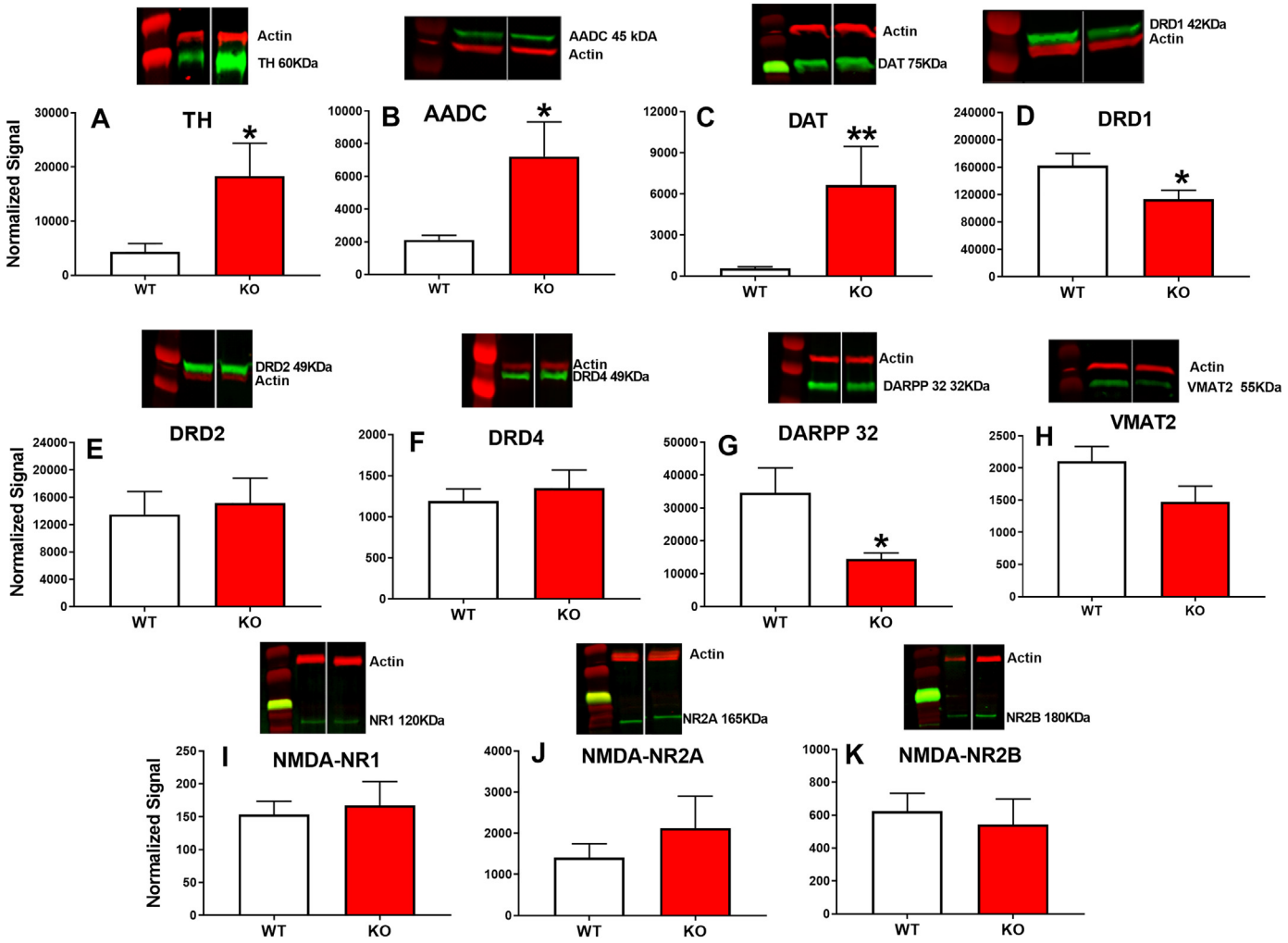

Fig. 4. Striatal DA and NMDA markers. Western blot analyses showed that *Lphn3* KO rats have increased expression of TH, AADC, and DAT (A-C) and decreased expression of DRD1 and DARPP-32 (D, G) compared with WT littermates. Group sizes KO: $n = 6$; WT: n = 6 (females). There were no significant changes in DRD2, DRD4, NMDA-NR1, -NR2A, or NR2-B (E, F, H, I, J, K respectively). *$p \leq .05$; ** $p \leq .01$ compared with WT rats.

activity the Genotype main effect was significant ($F(1,32.8) = 11.83$, $p < .01$). There was also a Genotype × Sex interaction ($F(1,32.8) = 8.39$, $p < .01$). Slice-effect ANOVAs by sex showed that the effects were significant for females ($p < .0001$ (Fig. 7A)) but not for males (Fig. 7C). Female KO rats were more active than WT females. For peripheral activity the main effect of genotype was not significant but the genotype × sex interaction was ($F(1,32.4) = 4.83$, $p < .05$; Fig. 7B & D). However, slice-effect ANOVAs on each sex both fell short of significance (females $p = .11$; males $p = .15$).

For central activity after saline injection, Genotype ($F(1,32.2) = 13.49$, $p < .001$), Genotype × Sex ($F(1,32.2) = 7.11$, $p < .02$), and Genotype × Interval ($F(2,44.2) = 5.25$, $p < .01$) were significant. Slice-effect ANOVAs on each sex showed the effect was significant in females ($p < .0001$) but not in males. Slice-effect ANOVAs on each interval showed effects in females at all intervals but no difference between males (Fig. 7A, C). For peripheral activity, the main effect of genotype was not significant but there was a genotype × sex interaction trend ($F(1,31.2) = 3.54$, $p = .069$; Fig. 7B, D).

After amphetamine all groups showed an increase in activity. For central activity, there was a main effect trend ($F(1,40.6) = 2.69$, $p = .10$) and a significant genotype × sex interaction ($F(1,40.6) = 5.65$, $p < .03$). Slice-effect ANOVAs by sex showed a significant effect in females ($p < .01$; Fig. 7A) but not males (Fig. 7C). Female KO rats were more active than WT females, a difference not seen in males. For peripheral activity, the main effect of genotype was not significant but there was a genotype × sex interaction ($F(1,41.7) = 9.18$, $p < .01$). Slice-effect ANOVAs by sex showed a significant effect in females ($F(1,41.7) = 10.34$, $p < .01$; Fig. 7B) but not in males (Fig. 7D). Female KO rats were more active than female WT rats.

When activity was analyzed as a percent of pre-drug baseline, there was a significant main effect of genotype ($F(1,35.6) = 4.98$, $p < .05$). The effect is shown in Fig. 8 by sex for consistency with the data in Fig. 7. The main effect is shown by the bracket connecting males and females (Fig. 8A, C). KO rats had less central activity relative to their higher pre-drug baseline compared with WT rats that had more central activity relative to their lower pre-drug baseline. For peripheral activity as percent of pre-drug baseline, the main effect of genotype was not significant however the genotype × sex interaction was ($F(1,36.5) = 4.08$, $p = .05$). Slice-effect ANOVAs by sex showed a significant effect in females ($p < .05$; Fig. 8B) but not in males (Fig. 8D). Interestingly, while the KO female central activity was less than WT females relative to their baselines, the KO females had more peripheral activity than WT females relative to their baselines (cf., Fig. 8A vs. 8B). For males, KO male post-drug relative change in activity was less in both the central and peripheral regions compared with WT males. This unusual pattern will be the subject of future experiments.

3.4.1. Monoamines

Monoamine and major metabolites were assayed in PFC, STR, NAcc,

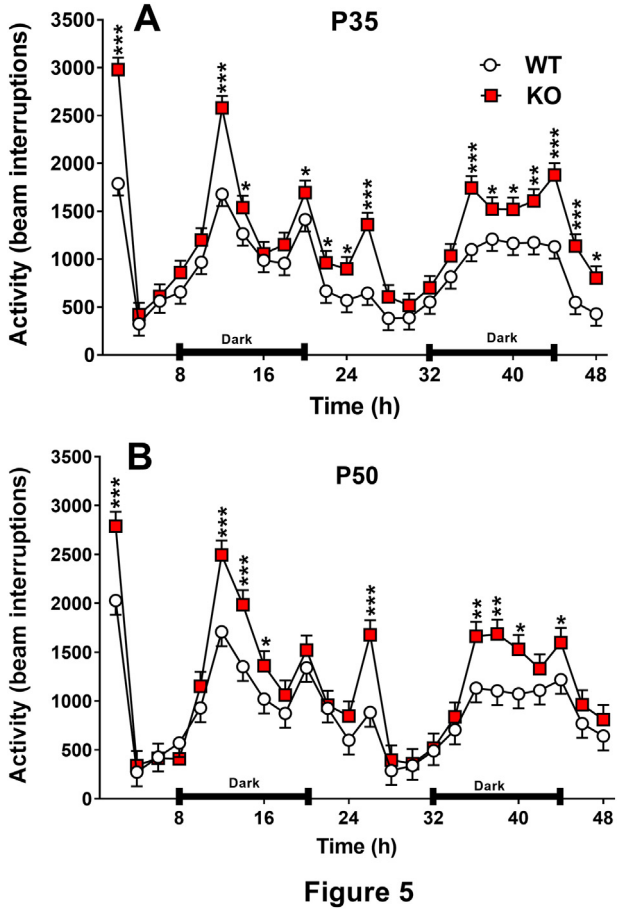

Fig. 5. Home-cage locomotor activity. Rats were tested in home-cage activity monitors for 48 h, starting 8 h before the start of the dark cycle and continuing through 2 dark cycles, one full light cycle and two partial light cycles, one at the beginning and one at the end. The vivarium was on a 14 h light, 10 h dark cycle. *A*, activity starting on P35. *B*, activity starting on P50. At both ages KO rats were hyperactive when first placed in the test. As both groups habituated, the higher activity of KO rats disappeared. Six hours into the first dark cycle, hyperactivity in KO rats reemerged and remained during most of the dark phase. At P35 KO hyperactivity continued during the second light phase then disappeared as habituation continued, reemerging a second time 6 h into the second dark phase, slowly dissipating during the last light phase. At P50 the dark cycle hyperactivity in the KO rats disappeared earlier than at P35, becoming non-significant during the last 4 h of the dark cycle. At this age there was a brief spike in activity in the KO rats 6 h into the light cycle, then disappeared again. During the second dark cycle, hyperactivity reappeared again 6 h into the dark phase. At this age the KO rats' hyperactivity disappeared as soon as the last light cycle began. Data are Mean ± SEM. Since there was no genotype × sex interaction, sexes are shown combined. Group sizes: P35: Male: WT n = 19, KO n = 19 Female: WT n = 19, KO = 19; P50: Male: WT n = 19, KO n = 19 Female: WT n = 19, KO = 19. Male: WT n = 19, KO n = 20; female: WT n = 20, KO n = 20. *p ≤ .05; **p ≤ .01, ***p < .001 vs. WT.

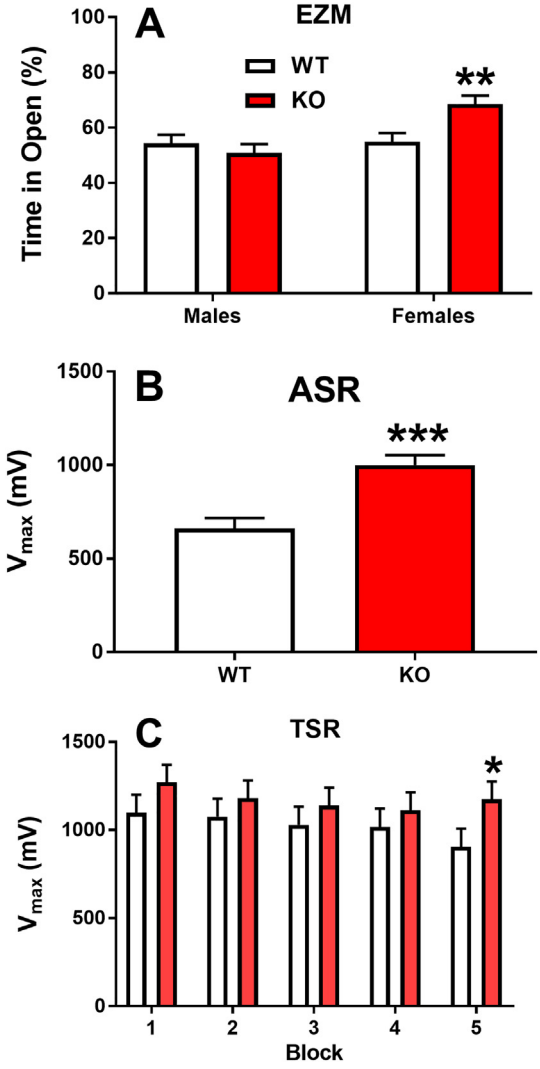

Fig. 6. Elevated zero-maze (EZM), acoustic startle response (ASR), and tactile startle response (TSR). In the EZM, KO females spent a larger percentage of their time in open quadrants compared with WT females. Males showed no differences (*A*). For ASR, regardless of sex, KO rats had significantly increased peak responses compared with WT rats (*B*). For TSR, KO rats had higher peak responses compared with WT rats, but the effect was only significant for block-5 (C). Group sizes: EZM: Males: WT n = 19, KO n = 20; females: WT n = 20, KO n = 20. ASR/TSR: WT n = 37, KO n = 36. *p ≤ .05;**p ≤ .01; ***p ≤ .001 vs. WT.

HIP, and Cb. No genotype-related differences were seen for NE, DOPAC, DA, 5-HIAA, HVA, or 5-HT in any region (Table 2).

4. Discussion

Latrophilin orthologues are found in all animals with at least three homologues present in chordates (Fredriksson and Schioth, 2005; Nordstrom et al., 2009). They are also conserved in invertebrates with expression in the nervous system (Rohou et al., 2007). LPHN3 is found in insects, invertebrates, and vertebrates, yet it remains poorly understood. LPHN3 is a synaptic adhesion GPCR with an extracellular domain that binds to FLRT3 and tenurin-3 to span the synapse and has a Gq/11 intracellular domain hypothesized to regulate neurotransmitter release (Davletov et al., 1998; Sugita et al., 1998; Ichtchenko et al., 1999). There is evidence that it plays a role in brain development; its concentrations are highest early in development and gradually decline to stable adult levels (Arcos-Burgos and Muenke, 2010). There are 21 *LPHN3* variants linked with ADHD, but how each contributes to symptoms is unknown. Transgenic models of LPHN3 disruption in *Drosophila*, zebrafish, and mouse have been reported (Lange et al., 2012; Wallis et al., 2012; Orsini et al., 2016; van der Voet et al., 2016; Lange et al., 2018). All are consistent in demonstrating that LPHN3 disruption results in hypermobility. We created a rat model to investigate this poorly understood protein and its relationship to hyperactivity. Rats have several advantages over these other species that may be useful for understanding what this protein does under normal and abnormal conditions. Rats have a greater range of behavioral capacities than mice and may ultimately be used to investigate other attributes of ADHD, such as inattention, impulsivity, and cognitive effects. As the

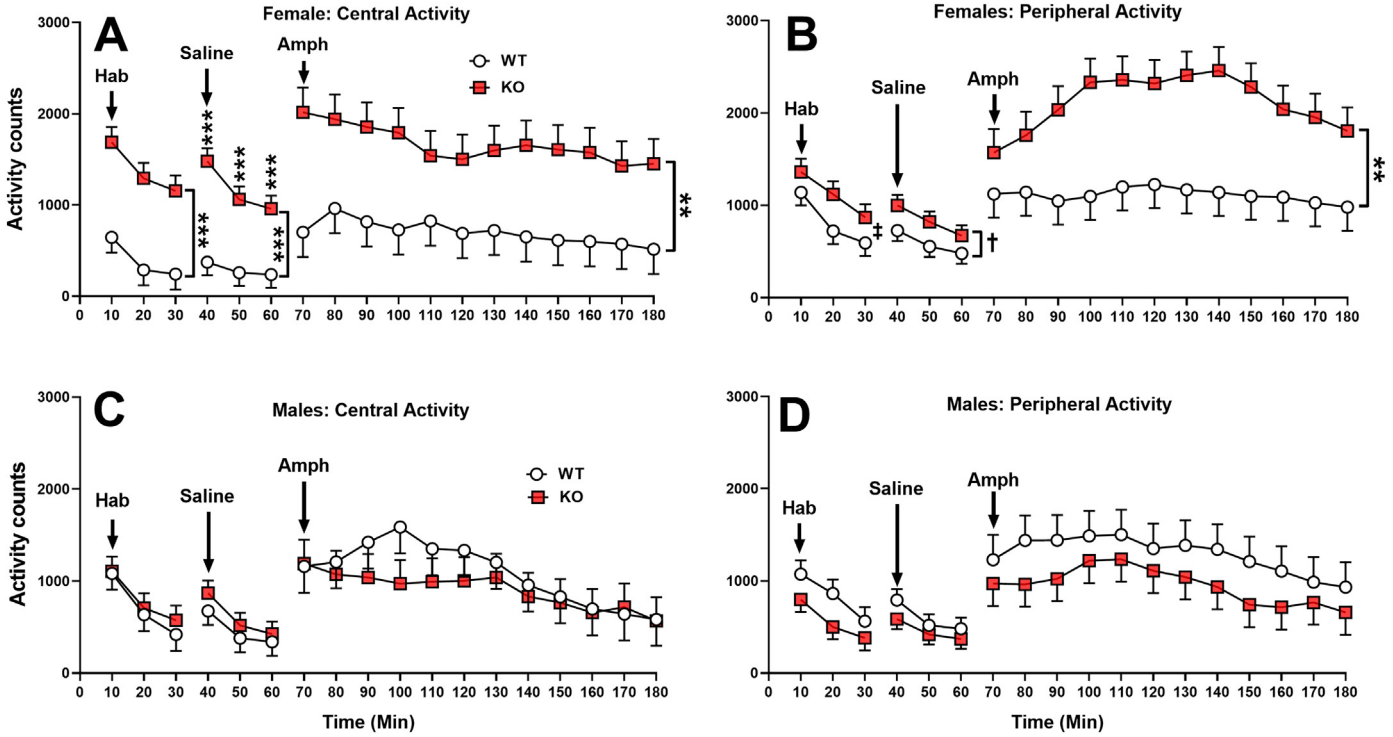

Fig. 7. Open-field activity habituation (2 phases) and after amphetamine challenge: Untreated KO and WT rats were first habituated to the test arena for 30 min (Hab), removed, injected with saline and tested for another 30 min (Saline); they were then removed a second time and injected with 1 mg/kg (+) amphetamine and tested for another 120 min (Amph). KO rats, predominately females, were hyperactive during the untreated habituation and saline habituation periods, and even more hyperactive after amphetamine in both the central region (*A*) and peripheral area (*B*) compared with males in the central region (*C*) or peripheral area (*D*). Group sizes: Male: WT $n = 12$, KO $n = 10$ Female: WT $n = 13$, KO $= 10$. **p ≤ .01; ***p ≤ .001, $^{\dagger}p \leq .10$; $^{\ddagger}p = .11$ vs WT.

first report of the rat KO of LPHN3, the objective here was first to establish the hyperactive phenotype and the rat KO shows several features not seen in the most closely related model, the *Lphn3* KO mouse. For example, the KO rat was hyperactive in two different familiar environments, home-cage and after habituation to an open-field. This was not shown for the KO mouse. The KO rat is hyper-reactive as seen in tests of acoustic startle, the mouse KO has no report on acoustic startle. The rat KO, mostly in females, shows a reduction in activity after challenged with a sympathomimetic stimulant, amphetamine, relative to its pre-drug activity level, unlike WT controls that do not show such a pattern. By contrast, the KO mouse shows exaggerated hyperactivity in response to the sympathomimetic stimulant, cocaine. Female KO rats also showed increased time-in-open in the elevated zero-maze test of anxiety-like behavior without an increase in number of quadrant entries suggesting that the effect was not a byproduct of being hyperactive.

Additionally, KO rats showed changes in striatal markers of dopamine regulation. These included increased TH, AADC, and DAT accompanied by decreased DRD1 and DARPP32 by western analysis, with no changes in related gene expression or protein levels for *Lphn1*/LPHN1, *Lphn2*/LPHN2, or *Flrt3*/FLRT3 in striatum. Nor was gene expression of these factors changed in PFC or for *Lphn2* or *Flrt3* in hippocampus with a minor reduction in *Lphn1* in hippocampus, demonstrating the selectivity of the rat KO while not affecting related genes or proteins.

We also obtained all rats for testing using heterozygotes crossing to avoid issues from null × null vs. WT × WT crosses. We controlled for litter effects by selecting only one male and one female of each genotype from each litter (Crusio, 2004; Crusio et al., 2009) and also used litter as a random factor in ANOVA mixed linear models to ensure litter contributions were accounted for in the statistical analyses (Holson and Pearce, 1992; Lazic and Essioux, 2013; Williams et al., 2017).

The *Lphn3* KO rat is not a model of ADHD per se because in humans *LPHN3* variants lead to reduced gene expression, not a null genotype (Domene et al., 2011; Martinez et al., 2016). Our objective was to use a loss-of-function model to better understand the function of LPHN3. Given that LPHN3 was suggested to have effects on activity, we assessed locomotor activity in familiar environments (hyperactivity is a characteristic of ADHD in familiar environments) and after a challenge dose with amphetamine (a drug used to treat ADHD), and we found effects consistent with ADHD. Because ADHD is associated with changes in DA signaling and because there is cross-talk between DA and NMDA-Rs we also examined NMDA-NR1, -NR2A, and –NR2B in striatum and found no differences in KO rats. But, we saw no changes in levels of DA, NE, 5-HT or their major metabolites by HPLC-ECD in relevant brain regions (STR, HIP, or PFC).

Lphn3 KO rats of both sexes were hyperactive. This was most pronounced during the dark phase in the home-cage test. The hyperactivity was present at P35 and at P50. In an open-field even after an hour of no-treatment and saline-treatment habituation, KO rats remained hyperactive. After amphetamine, however, complex changes were seen in males versus females. The basis of these differential responses are not yet known and require further investigation. Interestingly, children with ADHD also show a decline in hyperactivity relative to their level before treatment (Labbe et al., 2012; Briars and Todd, 2016) as do the KO rats.

Sex differences in ADHD prevalence in humans are well documented. ADHD affects 5–7% of the school age children, with a male to female ratio of ~3:1 (Willcutt, 2012; Arnett et al., 2015). Males are more often diagnosed with the combined or impulsive subtype of ADHD, whereas females are more often diagnosed with the inattentive subtype (Gaub and Carlson, 1997). One hypothesis to explain these differences is that females internalize and become more easily distracted whereas males with ADHD are hyperactive and impulsive because they tend toward externalized behavior (Arnold, 1996; Biederman et al., 1999; Quinn, 2008).

Combining the behavioral and neurochemical data suggest that

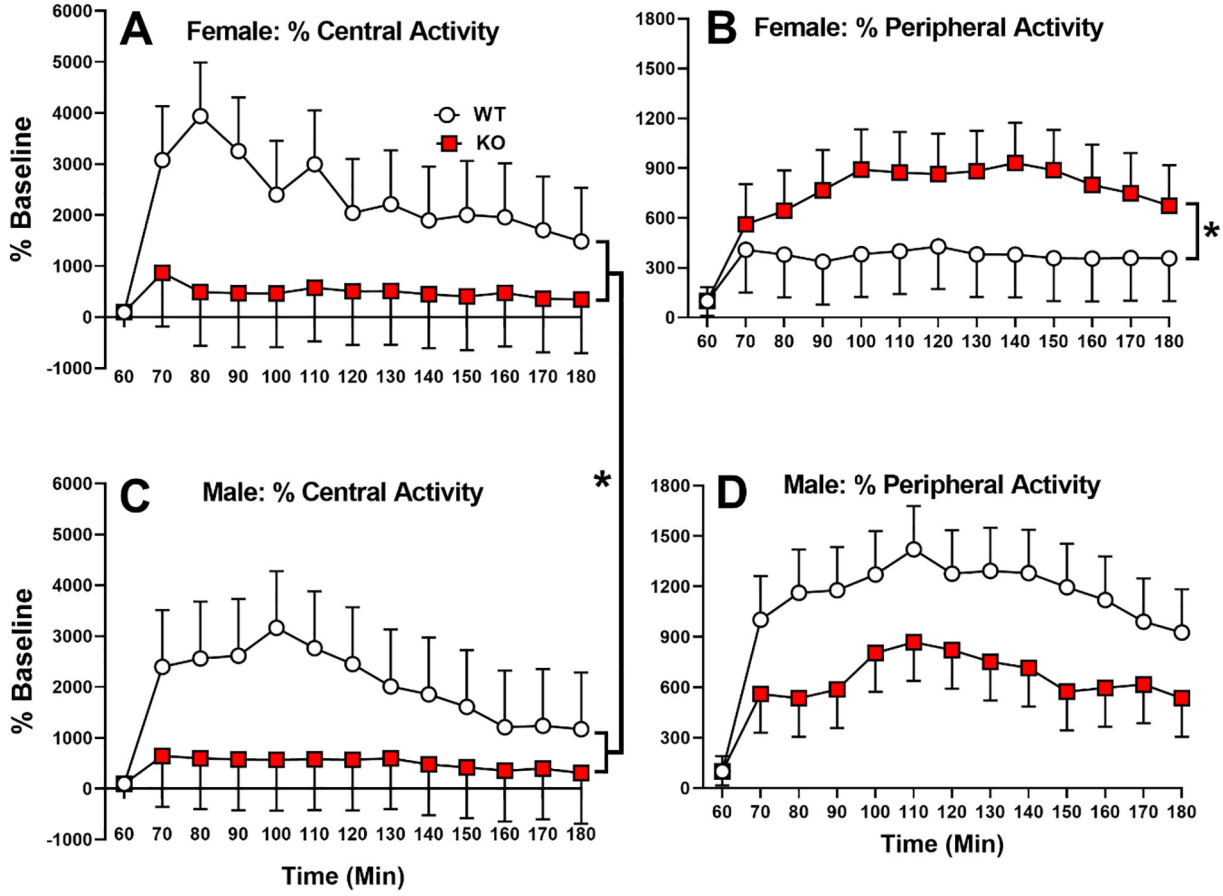

Fig. 8. Open-field percent change in activity after amphetamine relative to each groups' pre-drug baseline. *A*, Female central activity percent change. *B*, Female peripheral activity percent change. *C*, Male central activity percent change. *D*, Male peripheral activity percent change. Group sizes: same as in Fig. 7. *p ≤ .05 vs. WT.

increased DA synthesis may result in DA overflow leading to DA-mediated hyperlocomotion. If DA release in STR is increased, this would be consistent with the altered response to amphetamine. Hence, the data point toward LPHN3 having a role in striatal DA regulation. These effects are in general agreement with the mouse, *Drosophila,* and zebrafish models of disrupted brain LPHN3 and with the human reduction in *LPHN3* expression in some children with ADHD.

While both the rat and mouse KO models show hyperactivity, they also differ. The *Lphn3* KO mouse shows increased levels of brain DA, NE, and 5-HT whereas the KO rat does not. The KO mouse had no working memory or discrimination deficits in an operant task, but showed higher lever press rates on a high FR schedule (40:1); we have not tested the KO rat for schedule controlled behavior. KO mice show less immobility in a forced swim test, a behavior we did not test in KO rats but may also reflect the KO hyperactivity effect. In primary neuronal culture, KO mice showed increased neurite outgrowth, reduced transcripts for cell adhesion and calcium signaling proteins, consistent with LPHN3 being an adhesion protein, we have not examined these factors.

The largest effect in LPHN3 KO rats was nocturnal hyperactivity; this was seen at both adolescent and adult ages, demonstrating persistence. ADHD patients show hyperactivity in familiar settings (Sagvolden and Sergeant, 1998) and as KO rats habituated to the home-cage environment their hyperactivity dissipated at first, then re-emerged with a delayed onset of about 6 h during the dark cycle. Rodent activity typically peaks 5–6 h into the night phase (Zoratto et al., 2013) and this peak was heightened in KO rats. Once it emerged, hyperactivity continued for the remainder of the dark cycle in KO rats, then dissipated again during the next light period and reemerged 6 h into the second dark period.

Lphn3 KO rats showed facilitated acoustic and tactile startle. Appropriate filtering of stimuli is a critical component of attention. To further assess this, we plan to assess prepulse inhibition of acoustic startle, a measure of sensorimotor gating in follow-up experiments. Patients with ADHD report being flooded with sensory stimuli, an effect that can cause increased reactivity (Faraone et al., 2000), and there are data indicating sensory processing deficits in those with ADHD (Durukan et al., 2008; Holstein et al., 2013; Micoulaud-Franchi et al., 2015).

Dysregulated monoaminergic systems are seen in ADHD and treatment of ADHD with psychostimulants that increase or prolong catecholamine release provide clinical benefit (Zhu and Reith, 2008; dela Pena et al., 2015). Abnormal monoamine synthesis is also reported in patients with ADHD (Ernst et al., 1998; Ernst et al., 1999), consistent with our KO rat finding of increased TH and AADC levels (Cook Jr. et al., 1995; LaHoste et al., 1996; Gill et al., 1997).

ADHD is a polygenic disorder, with multiple small effect genes contributing in yet to be defined combinations along with unknown environmental contributions. Moreover, ADHD is a set of traits along a continuum (Akutagava-Martins et al., 2016) and cannot be modeled by any single-gene effect. However, genes that confer ADHD risk need to be disentangled and this can be done by dissecting the effects of each genetic contribution. *LPHN3* is not a dominant variant but contributes to a subset of ADHD cases in conjunction with other gene variants. Hence, *Lphn3* variants confer incremental risk but are not a cause of ADHD. Nevertheless, LPHN3 may be a potential target for drug development for those that carry an *LPHN3* risk allele.

Table 2
Regional brain monoamine concentrations.

PFC		
Monoamine	WT	KO
NE	317.6 (24.3)	282.8 (23.8)
5-HIAA	1368.8 (95.9)	1378.7 (97.5)
5-HT	1510 (22.5)	1408.8 (22.6)
STR		
	WT	KO
NE	109.6 (14.0)	114.9 (13.7)
DOPAC	1404.2 (181.1)	1503.5 (173.9)
DA	4706.1 (625.4)	4185.7 (614.1)
5-HIAA	1103.6 (78.4)	989.2 (77.3)
HVA	439.2 (51.1)	526.9 (53.2)
5-HT	803.0 (76.3)	688.5 (72.6)
NAcc		
	WT	KO
NE	1140.8 (168.6)	1159.5 (157.7)
DOPAC	951.1 (172.8)	1038.0 (164.7)
DA	2318.8 (412.8)	2520.3 (412.4)
5-HIAA	1604.7 (82.0)	1544.4 (75.8)
HVA	262.7 (44.3)	238.9 (38.6)
5-HT	1509.8 (160.4)	1408.8 (157.4)
HIP		
Monoamine	WT	KO
NE	312.14 (21.9)	353.7 (20.0)
5-HIAA	866.2 (38.4)	886.1 (36.8)
5-HT	464.1 (71.7)	441.3 (95.8)
Cb		
	WT	KO
NE	210.67 (9.7)	180.02 (9.2)
DOPAC	60.4 (6.2)	51.3 (5.6)
5-HIAA	179.5 (10.5)	157.9 (10.5)
5-HT	113.8 (12.9)	116.0 (12.5)

Values are Mean (SEM) (pg/mg tissue).
WT: $n = 16$, KO: $n = 16$.

Acknowledgement

This research was supported by a grant from the L.I.F.E. Foundation and NIH T32 ES007051 (E.M.P.) and these institutional shared services: Transgenic Animal and Genome Editing Core and Animal Behavior Core, Cincinnati Children's Research Foundation.

Conflict of interest statement

The authors declare no conflict of interest.

References

Silva, J.P., Ushkaryov, Y.A., 2010. The latrophilins, "split-personality" receptors. Adv. Exp. Med. Biol. 706, 59–75.
Acosta, M.T., Velez, J.I., Bustamante, M.L., Balog, J.Z., Arcos-Burgos, M., Muenke, M., 2011. A two-locus genetic interaction between LPHN3 and 11q predicts ADHD severity and long-term outcome. Transl. Psychiatry 1, e17.
Akutagava-Martins, G.C., Rohde, L.A., Hutz, M.H., 2016. Genetics of attention-deficit/hyperactivity disorder: an update. Expert. Rev. Neurother. 16, 145–156.
Arcos-Burgos, M., Muenke, M., 2010. Toward a better understanding of ADHD: LPHN3 gene variants and the susceptibility to develop ADHD. Attention Deficit Hyperactivity Disord. 2, 139–147.
Arcos-Burgos, M., et al., 2010. A common variant of the latrophilin 3 gene, LPHN3, confers susceptibility to ADHD and predicts effectiveness of stimulant medication. Mol. Psychiatry 15, 1053–1066.
Arcos-Burgos, M., et al., 2019. ADGRL3 (LPHN3) variants predict substance use disorder. Transl. Psychiatry 9, 42.
Arnett, A.B., Pennington, B.F., Willcutt, E.G., DeFries, J.C., Olson, R.K., 2015. Sex differences in ADHD symptom severity. J. Child Psychol. Psychiatry Allied Discip. 56, 632–639.
Arnold, L.E., 1996. Sex differences in ADHD: conference summary. J. Abnorm. Child Psychol. 24, 555–569.
de Bartolomeis, A., Buonaguro, E.F., Iasevoli, F., Tomasetti, C., 2014. The emerging role of dopamine-glutamate interaction and of the postsynaptic density in bipolar disorder pathophysiology: implications for treatment. J. Psychopharmacol. 28, 505–526.
Biederman, J., Faraone, S.V., Mick, E., Williamson, S., Wilens, T.E., Spencer, T.J., Weber, W., Jetton, J., Kraus, I., Pert, J., Zallen, B., 1999. Clinical correlates of ADHD in females: findings from a large group of girls ascertained from pediatric and psychiatric referral sources. J. Am. Acad. Child Adolesc. Psychiatry 38, 966–975.
Briars, L., Todd, T., 2016. A review of pharmacological Management of Attention-Deficit/hyperactivity disorder. JPPT 21, 192–206.
Cook Jr., E.H., Stein, M.A., Krasowski, M.D., Cox, N.J., Olkon, D.M., Kieffer, J.E., Leventhal, B.L., 1995. Association of attention-deficit disorder and the dopamine transporter gene. Am. J. Hum. Genet. 56, 993–998.
Crusio, W.E., 2004. Flanking gene and genetic background problems in genetically manipulated mice. Biol. Psychiatry 56, 381–385.
Crusio, W.E., Goldowitz, D., Holmes, A., Wolfer, D., 2009. Standards for the publication of mouse mutant studies. Genes Brain Behav. 8, 1–4.
Davletov, B.A., Meunier, F.A., Ashton, A.C., Matsushita, H., Hirst, W.D., Lelianova, V.G., Wilkin, G.P., Dolly, J.O., Ushkaryov, Y.A., 1998. Vesicle exocytosis stimulated by alpha-latrotoxin is mediated by latrophilin and requires both external and stored Ca2+. EMBO J. 17, 3909–3920.
Demontis, D., et al., 2019. Discovery of the first genome-wide significant risk loci for attention deficit/hyperactivity disorder. Nat. Genet. 51, 63–75.
Domene, S., Stanescu, H., Wallis, D., Tinloy, B., Pineda, D.E., Kleta, R., Arcos-Burgos, M., Roessler, E., Muenke, M., 2011. Screening of human LPHN3 for variants with a potential impact on ADHD susceptibility. Am. J. Med. Genet. B Neuropsychiatr. Genet. 156b, 11–18.
Durukan, I., Turkbay, T., Congologlu, A., 2008. The effects of methylphenidate on various components of visual attention in children with attention-deficit hyperactivity disorder. Turk psikiyatri dergisi 19, 358–364.
Ernst, M., Zametkin, A.J., Matochik, J.A., Jons, P.H., Cohen, R.M., 1998. DOPA decarboxylase activity in attention deficit hyperactivity disorder adults. A [fluorine-18] fluorodopa positron emission tomographic study. J. Neurosci. 18, 5901–5907.
Ernst, M., Zametkin, A.J., Matochik, J.A., Pascualvaca, D., Jons, P.H., Cohen, R.M., 1999. High midbrain [18F]DOPA accumulation in children with attention deficit hyperactivity disorder. Am. J. Psychiatry 156, 1209–1215.
Faraone, S.V., Biederman, J., Spencer, T., Wilens, T., Seidman, L.J., Mick, E., Doyle, A.E., 2000. Attention-deficit/hyperactivity disorder in adults: an overview. Biol. Psychiatry 48, 9–20.
Franke, B., Faraone, S.V., Asherson, P., Buitelaar, J., Bau, C.H., Ramos-Quiroga, J.A., Mick, E., Grevet, E.H., Johansson, S., Haavik, J., Lesch, K.P., Cormand, B., Reif, A., 2012. The genetics of attention deficit/hyperactivity disorder in adults, a review. Mol. Psychiatry 17, 960–987.
Fredriksson, R., Schioth, H.B., 2005. The repertoire of G-protein-coupled receptors in fully sequenced genomes. Mol. Pharmacol. 67, 1414–1425.
Gaub, M., Carlson, C.L., 1997. Gender differences in ADHD: a meta-analysis and critical review. J. Am. Acad. Child Adolesc. Psychiatry 36, 1036–1045.
Gill, M., Daly, G., Heron, S., Hawi, Z., Fitzgerald, M., 1997. Confirmation of association between attention deficit hyperactivity disorder and a dopamine transporter polymorphism. Mol. Psychiatry 2, 311–313.
Holson, R.R., Pearce, B., 1992. Principles and pitfalls in the analysis of prenatal treatment effects in multiparous species. Neurotoxicol. Teratol. 14, 221–228.
Holstein, D.H., Vollenweider, F.X., Geyer, M.A., Csomor, P.A., Belser, N., Eich, D., 2013. Sensory and sensorimotor gating in adult attention-deficit/hyperactivity disorder (ADHD). Psychiatry Res. 205, 117–126.
Huang, X., Zhang, Q., Gu, X., Hou, Y., Wang, M., Chen, X., Wu, J., 2018. LPHN3 gene variations and susceptibility to ADHD in Chinese Han population: a two-stage case-control association study and gene-environment interactions.
Hwang, I.W., Lim, M.H., Kwon, H.J., Jin, H.J., 2015. Association of LPHN3 rs6551665 a/G polymorphism with attention deficit and hyperactivity disorder in Korean children. Gene 566, 68–73.
Ichtchenko, K., Bittner, M.A., Krasnoperov, V., Little, A.R., Chepurny, O., Holz, R.W., Petrenko, A.G., 1999. A novel ubiquitously expressed alpha-latrotoxin receptor is a member of the CIRL family of G-protein-coupled receptors. J. Biol. Chem. 274, 5491–5498.
Labbe, A., Liu, A., Atherton, J., Gizenko, N., Fortier, M.E., Sengupta, S.M., Ridha, J., 2012. Refining psychiatric phenotypes for response to treatment: contribution of LPHN3 in ADHD. Am. J. Med. Genet. B Neuropsychiatr. Genet. 159B, 776–785.
LaHoste, G.J., Swanson, J.M., Wigal, S.B., Glabe, C., Wigal, T., King, N., Kennedy, J.L., 1996. Dopamine D4 receptor gene polymorphism is associated with attention deficit hyperactivity disorder. Mol. Psychiatry 1, 121–124.
Lange, M., Norton, W., Coolen, M., Chaminade, M., Merker, S., Proft, F., Schmitt, A., Vernier, P., Lesch, K.P., Bally-Cuif, L., 2012. The ADHD-susceptibility gene lphn3.1 modulates dopaminergic neuron formation and locomotor activity during zebrafish development. Mol. Psychiatry 17, 946–954.
Lange, M., Froc, C., Grunwald, H., Norton, W.H.J., Bally-Cuif, L., 2018. Pharmacological analysis of zebrafish lphn3.1 morphant larvae suggests that saturated dopaminergic signaling could underlie the ADHD-like locomotor hyperactivity. Prog. Neuro-Psychopharmacol. Biol. Psychiatry 84, 181–189.

Lazic, S.E., Essioux, L., 2013. Improving basic and translational science by accounting for litter-to-litter variation in animal models. BMC Neurosci. 14, 37.
Livak, K.J., Schmittgen, T.D., 2001. Analysis of relative gene expression data using real-time quantitative PCR and the 2(−Delta Delta C(T)) Method. Methods (San Diego, Calif.) 25, 402–408.
Martinez, A.F., Muenke, M., Arcos-Burgos, M., 2011. From the black widow spider to human behavior: Latrophilins, a relatively unknown class of G protein-coupled receptors, are implicated in psychiatric disorders. Am. J. Med. Genet. B Neuropsychiatr. Genet. 156B, 1–10.
Martinez, A.F., Abe, Y., Hong, S., Molyneux, K., Yarnell, D., Löhr, H., Driever, W., Acosta, M.T., Arcos-Burgos, M., Muenke, M., 2016. An Ultraconserved brain-specific enhancer within ADGRL3 (LPHN3) underpins attention-deficit/hyperactivity disorder susceptibility. Biol. Psychiatry 80, 943–954.
Micoulaud-Franchi, J.A., Lopez, R., Vaillant, F., Richieri, R., El-Kaim, A., Bioulac, S., Philip, P., Boyer, L., Lancon, C., 2015. Perceptual abnormalities related to sensory gating deficit are core symptoms in adults with ADHD. Psychiatry Res. 230, 357–363.
Nordstrom, K.J., Lagerstrom, M.C., Waller, L.M., Fredriksson, R., Schioth, H.B., 2009. The secretin GPCRs descended from the family of adhesion GPCRs. Mol. Biol. Evol. 26, 71–84.
Olincy, A., Ross, R.G., Harris, J.G., Young, D.A., McAndrews, M.A., Cawthra, E., McRae, K.A., Sullivan, B., Adler, L.E., Freedman, R., 2000. The P50 auditory event-evoked potential in adult attention-deficit disorder: comparison with schizophrenia. Biol. Psychiatry 47, 969–977.
Orsini, C.A., Setlow, B., DeJesus, M., Galaviz, S., Loesch, K., Ioerger, T., Wallis, D., 2016. Behavioral and transcriptomic profiling of mice null for Lphn3, a gene implicated in ADHD and addiction. Mol. Genet. Genomic Med. 4, 322–343.
O'Sullivan, M.L., Martini, F., von Daake, S., Comoletti, D., Ghosh, A., 2014. LPHN3, a presynaptic adhesion-GPCR implicated in ADHD, regulates the strength of neocortical layer 2/3 synaptic input to layer 5. Neural Dev. 9, 7.
dela Pena, I., Gevorkiana, R., Shi, W.X., 2015. Psychostimulants affect dopamine transmission through both dopamine transporter-dependent and independent mechanisms. Eur. J. Pharmacol. 764, 562–570.
Quinn, P.O., 2008. Attention-deficit/hyperactivity disorder and its comorbidities in women and girls: an evolving picture. Curr. Psychiatry Rep. 10, 419–423.
Ranaivoson, F.M., Liu, Q., Martini, F., Bergami, F., von Daake, S., Li, S., Lee, D., Demeler, B., Hendrickson, W.A., Comoletti, D., 2015. Structural and mechanistic insights into the Latrophilin3-FLRT3 complex that mediates glutamatergic synapse development. Structure 23, 1665–1677.
Ribases, M., Ramos-Quiroga, J.A., Sanchez-Mora, C., Bosch, R., Richarte, V., Palomar, G., Gastaminza, X., Bielsa, A., Arcos-Burgos, M., Muenke, M., Castellanos, F.X., Cormand, B., Bayes, M., Casas, M., 2011. Contribution of LPHN3 to the genetic susceptibility to ADHD in adulthood: a replication study. Genes Brain Behav. 10, 149–157.
Rohou, A., Nield, J., Ushkaryov, Y.A., 2007. Insecticidal toxins from black widow spider venom. Toxicon 49, 531–549.
Russell, V.A., Sagvolden, T., Johansen, E.B., 2005. Animal models of attention-deficit hyperactivity disorder. Behav. Brain Funct. 1, 9.
Sagvolden, T., Sergeant, J.A., 1998. Attention deficit/hyperactivity disorder–from brain dysfunctions to behaviour. Behav. Brain Res. 94, 1–10.
Sagvolden, T., Aase, H., Zeiner, P., Berger, D., 1998. Altered reinforcement mechanisms in attention-deficit/hyperactivity disorder. Behav. Brain Res. 94, 61–71.
Sando, R., Jiang, X., Sudhof, T.C., 2019. Latrophilin GPCRs direct synapse specificity by coincident binding of FLRTs and teneurins. Science 363.
Scott, M.A., Hu, Y.C., 2019. Generation of CRISPR-edited rodents using a Piezo-driven zygote injection technique. Methods Mol. Biol. (Clifton, NJ) 1874, 169–178.
Steinberg, E.A., Drabick, D.A., 2015. A developmental psychopathology perspective on ADHD and comorbid conditions: the role of emotion regulation. Child Psychiatry Hum. Dev. 46, 951–966.
Sugita, S., Ichtchenko, K., Khvotchev, M., Sudhof, T.C., 1998. Alpha-Latrotoxin receptor CIRL/latrophilin 1 (CL1) defines an unusual family of ubiquitous G-protein-linked receptors. G-protein coupling not required for triggering exocytosis. J. Biol. Chem. 273, 32715–32724.
Tang, X., Orchard, S.M., Sanford, L.D., 2002. Home cage activity and behavioral performance in inbred and hybrid mice. Behav. Brain Res. 136, 555–569.
Tung, I., Li, J.J., Meza, J.I., Jezior, K.L., Kianmahd, J.S., Hentschel, P.G., O'Neil, P.M., Lee, S.S., 2016. Patterns of comorbidity among girls with ADHD: a meta-analysis. Pediatrics 138.
van der Voet, M., Harich, B., Franke, B., Schenck, A., 2016. ADHD-associated dopamine transporter, latrophilin and neurofibromin share a dopamine-related locomotor signature in Drosophila. Mol. Psychiatry 21, 565–573.
Vorhees, C.V., He, E., Skelton, M.R., Graham, D.L., Schaefer, T.L., Grace, C.E., Braun, A.A., Amos-Kroohs, R., Williams, M.T., 2011. Comparison of (+)-methamphetamine, +/− −methylenedioxymethamphetamine, (+)-amphetamine and +/− −fenfluramine in rats on egocentric learning in the Cincinnati water maze. Synapse (New York, NY) 65, 368–378.
Wallis, D., Hill, D.S., Mendez, I.A., Abbott, L.C., Finnell, R.H., Wellman, P.J., Setlow, B., 2012. Initial characterization of mice null for Lphn3, a gene implicated in ADHD and addiction. Brain Res. 1463, 85–92.
Willcutt, E.G., 2012. The prevalence of DSM-IV attention-deficit/hyperactivity disorder: a meta-analytic review. Neurotherapeutics 9, 490–499.
Williams, D.R., Carlsson, R., Burkner, P.C., 2017. Between-litter variation in developmental studies of hormones and behavior: inflated false positives and diminished power. Front. Neuroendocrinol. 47, 154–166.
Yang, H., Wang, H., Jaenisch, R., 2014. Generating genetically modified mice using CRISPR/Cas-mediated genome engineering. Nat. Protoc. 9, 1956–1968.
Zhang, L., Chang, S., Li, Z., Zhang, K., Du, Y., Ott, J., Wang, J., 2012. ADHDgene: a genetic database for attention deficit hyperactivity disorder. Nucleic Acids Res. 40, D1003–D1009.
Zhu, J., Reith, M.E., 2008. Role of the dopamine transporter in the action of psychostimulants, nicotine, and other drugs of abuse. CNS Neurol. Disord. Drug Targets 7, 393–409.
Zoratto, F., Tringle, A.L., Bellenchi, G., Speranza, L., Travaglini, D., di Porzio, U., Perrone-Capano, C., Laviola, G., Dreyer, J.L., Adriani, W., 2013. Impulsivity and home-cage activity are decreased by lentivirus-mediated silencing of serotonin transporter in the rat hippocampus. Neurosci. Lett. 548, 38–43.